Magnus Rogeberg
Tore Vehus
Lene Grutle
Tyge Greibrokk
Steven Ray Wilson
Elsa Lundanes

Department of Chemistry, University of Oslo, Blindern, Oslo, Norway

Received May 11, 2013
Revised May 31, 2013
Accepted May 31, 2013

Research Article

Separation optimization of long porous-layer open-tubular columns for nano-LC–MS of limited proteomic samples

The single-run resolving power of current 10 μm id porous-layer open-tubular (PLOT) columns has been optimized. The columns studied had a poly(styrene-co-divinylbenzene) porous layer (~0.75 μm thickness). In contrast to many previous studies that have employed complex plumbing or compromising set-ups, SPE–PLOT-LC-MS was assembled without the use of additional hardware/noncommercial parts, additional valves or sample splitting. A comprehensive study of various flow rates, gradient times, and column length combinations was undertaken. Maximum resolution for <400 bar was achieved using a 40 nL/min flow rate, a 400 min gradient and an 8 m long column. We obtained a 2.3-fold increase in peak capacity compared to previous PLOT studies (950 versus previously obtained 400, when using peak width = 2σ definition). Our system also meets or surpasses peak capacities obtained in recent reports using nano-ultra-performance LC conditions or long silica monolith nanocolumns. Nearly 500 proteins (1958 peptides) could be identified in just one single injection of an extract corresponding to 1000 BxPC3 beta catenin (−/−) cells, and ~1200 and 2500 proteins in extracts of 10 000 and 100 000 cells, respectively, allowing detection of central members and regulators of the Wnt signaling pathway.

Keywords: Nano-LC / Nanospray / Peak capacity / Porous layer open tubular columns / Wnt pathway
DOI 10.1002/jssc.201300499

Additional supporting information may be found in the online version of this article at the publisher's web-site

1 Introduction

Nano-LC–ESI-MS is commonly used for applications that require high sensitivity, as the narrow nanocolumns provide a higher concentration of eluting compounds. In addition, the low flow rates used in nano-LC can allow the whole eluate to enter the MS, thus increasing the sensitivity in ESI-MS [1, 2]. Further sensitivity improvements are desirable for the analysis of very limited samples, such as cancer stem cells, laser-capture microdissection samples or even single cells or cell components [3–5]. The sensitivity may be substantially increased by further downscaling column dimensions compared to the commonly used 75–50 μm id columns [2]. In addition to high sensitivity, a high resolving power is required to obtain maximum information from limited amounts of sample [6, 7]. Unlike packed and monolithic columns, the performance of open-tubular (OT) columns in LC is directly connected with the internal diameter, where narrower columns provide both higher analyte concentration in the eluate and higher efficiencies [8, 9]. Although OT-LC was introduced in 1978 [10], its use was limited by several obstacles such as extracolumn volumes, loadability, and the LODs of detectors [11, 12]. The loadability of OT columns was improved by introducing porous layers (PLOT columns) by etching silica [13, 14] and cross-linking polymeric layers [15]. Although OT-LC was already combined with MS in 1989 [16], a renewed interest in OT-LC began with the introduction of nano-electrospray in combination with OT columns [17]. Porous layer open tubular (PLOT) columns of 10 μm id with a 1 μm polymeric layer were used by Yue et al. for the separation of complex tryptic digests combined with nanospray ESI-MS [18], and was later found by our group to be well suited for intact protein separations [19]. PLOT-LC–MS has demonstrated subattomole LODs, high column-to-column repeatability, and high-resolving power [18, 19]. PLOT columns have also been combined on-line with precolumns for SPE and 2D

Correspondence: Magnus Rogeberg, Department of Chemistry, University of Oslo, Post Box 1033, Blindern, NO-0315 Oslo, Norway
E-mail: magnus.rogeberg@kjemi.uio.no
Fax: +47 22855441

Abbreviations: AIBN, azobisisobutyronitrile; **BMA-EDMA**, poly(butyl methacrylate-co-etylene dimethacrylate); **BuMa**, butyl methacrylate; **EDMA**, ethylene dimethacrylate; **EIC**, extracted ion chromatogram; **FA**, formic acid; **γ–MAPS**, 3-(trimethoxysilyl)propyl methacrylate; **OT**, open tubular; **PLOT**, porous-layer open-tubular; **PS-DVB**, poly(styrene-co-divinylbenzene); t_G, gradient time; $W_{0.1}$, peak width at 10 percent of peak height; $W_{0.5}$, peak width at half peak height; W_{av}, average peak width

LC [20]. In other words, there is great potential in the practical use of PLOT for, for example, bottom-up and top-down proteomics of limited samples. Although these PLOT columns themselves are remarkably simple to prepare, previously reported PLOT-LC systems typically require complicated set-ups with fittings that are not commercially available or require compromises such as sample splitting [19, 20], which can discourage analysts from exploring PLOT columns. Therefore, we have designed a simple SPE–PLOT-LC system that is fully compatible with commercial and automated nano-LC instrumentation, and that does not require extra hardware or custom-made parts (with the exception of the simply prepared columns). The columns used in this system were a 50 μm id methacrylate based monolithic precolumn and a 10 μm id poly(styrene-co-divinylbenzene) (PS-DVB) PLOT column.

As we are interested in obtaining the maximum resolution for our limited-sample applications, we decided to explore central chromatographic parameters to maximize the resolving power (flow rates, column length, gradient time (t_G), temperature, etc.), as detailed surveys of these parameters and their combinations have been missing regarding the separation power of modern PLOT columns.

2 Materials and methods

2.1 Materials and reagents

HPLC-grade acetonitrile (VWR, Radnor, PA, USA), type 1 (18.2 MΩ cm resistivity at 25°C) water produced with a Milli-Q water purification system (Merck Millipore, MA, USA) and formic acid (FA; Sigma-Aldrich, St. Louis, MO, USA) were used for the preparation of mobile phases. Divinylbenzene (DVB) 80% mixture of isomers, styrene (99%), the inhibitor 2,2-diphenyl-1-picrylhydrazyl, 3-(trimethoxysilyl)propyl methacrylate (γ–MAPS) (98%), butyl methacrylate (BuMa) (98%), 1,4-butanediol (99%), ethylene dimethacrylate (EDMA) (98%), anhydrous DMF (99.8%), azobisisobutyronitrile (AIBN), cytochrome c (12 kDa), and human transferrin (76–81 kDa) were purchased from Sigma-Aldrich. Polyimide-coated fused-silica tubes (365 μm od) were obtained from Polymicro Technologies (Phoenix, AZ, USA). 1-Propanol and NaOH pellets were purchased from Merck (Darmstadt, Germany). Ethanol was obtained from Arcus (Oslo, Norway). Nitrogen gas (99.99%) was purchased from AGA (Oslo, Norway).

2.2 Standard protein sample preparation

Human transferrin was reduced and alkylated using a previously described procedure [21]. Transferrin was dissolved in water to a concentration of 1 mg/mL. Denaturation and alkylation were done simultaneously by addition of 1 μg DL-dithiothreitol (DDT, Sigma-Aldrich) per 50 μg protein and incubation at 95°C for 15 min, followed by cooling to room temperature. Iodoacetamide (IAM, Sigma-Aldrich) was added (5 μg per 50 μg protein), and the sample was incubated in the dark at room temperature for 15 min. 5 μL 1 M triethylammonium bicarbonate buffer (pH 8.5, Sigma-Aldrich) and 5 μL 1 mg/mL trypsin (bovine pancreas, Sigma-Aldrich) solution were added to the 100 μL reduced and alkylated protein solution. Digestion was performed overnight at 37°C and stopped by adding 5 μL of FA.

100 μL of 1 mg/mL cytochrome c solution (aq) was added to 5 μL triethylammonium bicarbonate buffer (pH 8.5) and digested overnight at 37°C. The trypsination reaction was stopped by adding 5 μL FA. Transferrin and cytochrome c solutions were stored at 4°C until use.

2.3 Preparation of rat-liver extracts and BxPC3 samples

The in-gel-digested rat liver sample was prepared according to a previously described procedure [22]. In brief, 15 μL (40 μg/μL) of rat liver extract was loaded onto the gel. A slice containing the 50 kDa fraction was cut from the gel, containing about one-tenth of the total protein loaded. The sample was trypsinated overnight, extracted twice with 60 μL of 5% FA/acetonitrile (1:1, v/v) and then once with 60 μL of acetonitrile, followed by evaporation to dryness using a Savant Speedvac (Thermo Fischer) and stored at 4°C. Before injection, the sample was redissolved in 40 μL 0.1% (aq) FA and then the 1.5 μg/μL sample was further diluted using 3 μL of sample and 97 μL of water, to a final concentration of 45 ng/μL.

A β-catenin knock-out modified BxPC3 cell line was harvested and lysed in lysis buffer (Native lysis buffer, Cell Signaling, Danvers MA, USA) and 50 mM phenylmethylsulfonyl fluoride (Nigu Chemie, Germany) as described by the manufacturer to a final concentration of 100 000 cells/μL buffer. 20 μL of cell lysate was separated according to the manufacturer's protocol on an SDS-PAGE gel (3–8% Bis-TrisAcetate, NuPAGE, Invitrogen, Carlsbad, CA, USA) until sufficient (about 1 h at 150 V) separation was achieved. The gel was stained in Coomassie Blue, and excised in eight bands, which were digested with trypsin (Sequence Grade, Promega, Fitchburg, WI, USA) and extracted from the gel according to the manufacturer's protocol. The bands were pooled and the resulting sample dried in a Savant SpeedVac and diluted in 20 μL 0.1% v/v TFA (Sigma-Aldrich) in HPLC water (Sigma). Separation on a gel followed by in-gel digestion allowed efficient trypsination and removal of detergents from the lysis of the cells. For total sample analysis, the bands were pooled after digestion. The sample was further diluted with 0.1% v/v TFA to the desired concentrations.

2.4 Column preparation

The 10 μm id PLOT columns were prepared according to a previously described procedure [18], with the exception that

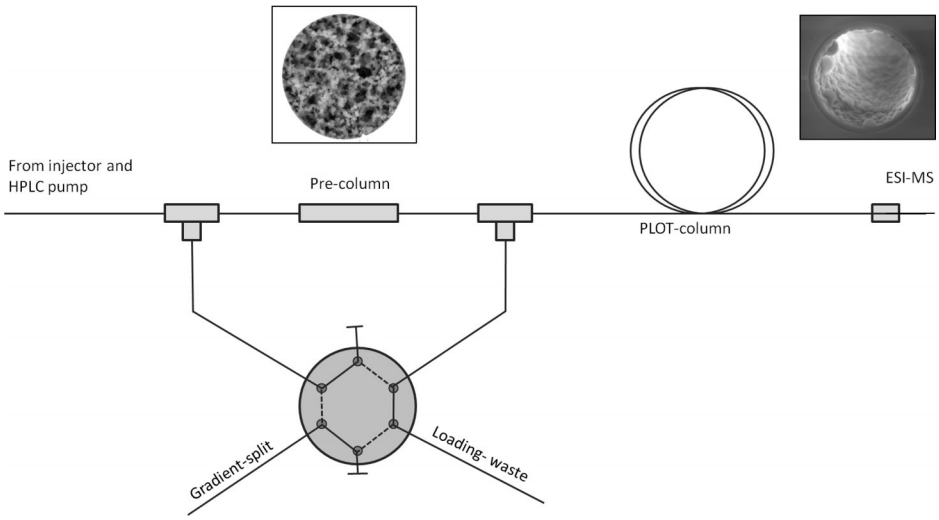

Figure 1. Schematic diagram of the column switching system. The entire 500 nL or 1 μL sample was loaded onto the 4.5 cm long 50 μm id BMA-EDMA monolithic precolumn at a flow rate of 0.5 μL/min for 2.5 min (solvent directed to loading waste). Following sample loading, the valve was switched and the flow rate was set to give 20–80 nL/min through the columns (see Section 2 for details). When the LC pump flow rate was stable, the gradient was started and the sample transferred to the PLOT column for separation and detection. The flow through the chromatographic system was determined by the backpressure over the chosen gradient-split capillary.

the ethanol to monomer ratio in the polymerization mixture was changed to reduce the column operational backpressure (see below). A simple homemade pressure bomb system coupled directly to a nitrogen flask was used for filling and washing the capillaries and columns (Supporting Information Fig. S1). A 50 or 10 μm id fused-silica capillary was cut to the desired length, and filled with aqueous 1 M NaOH solution, plugged with a rubber septum, and left in an oven at 100°C for 2 h. The capillaries were then flushed with water and acetonitrile and dried with nitrogen gas to remove residual water and acetonitrile, since the presence of water prevents the reaction between γ-MAPS and the silanol groups on the silica surface [23]. Silanization solutions were prepared from 5 mg 2,2-diphenyl-1-picrylhydrazyl dissolved in a mixture of 300 μL γ-MAPS and 700 μL anhydrous DMF, and filled in the pretreated capillaries. Both ends were plugged with a rubber septum, and the sealed capillary was left in an oven at 110°C for 6 h. After silanization the capillary was washed with acetonitrile and blown dry with nitrogen and subsequently filled with a polymerization mixture. Both the PLOT columns and the monolithic columns were prepared using the above described pretreatment and silanization procedure. For PLOT column preparation, the polymerization mixture consisted of 5 mg AIBN, 942 μL ethanol, 200 μL styrene, and 200 μL divinylbenzene. The polymerization solution was ultrasonicated for 5 min and filled in the pretreated 10 μm id capillary. Both ends of the capillary were plugged with a rubber septum and the capillary was placed in an oven at 74°C for 16 h. After polymerization, the column was washed with acetonitrile, dried with nitrogen, and both ends were inspected using an optical microscope (PME Olympus, Tokyo, Japan). With visual microscopic inspection of the PLOT columns, the columns were cut from both ends until a layer of polymer was seen inside (Supporting Information Fig. S2). After cutting 5–25 cm from both ends, the columns were ready for use. The 50 μm id poly(butyl methacrylate-co-EDMA) BMA-EDMA precolumn was made using a polymerization solution consisting of 269 μL BuMa, 152 μL EDMA, 423 μL 1-propanol, 256 μL 1,4-butanediol, and 41 mg AIBN, as previously described [24]. The prepared polymerization solution was degassed by ultrasonification for 5 min, filled in the silanized capillary and the ends were plugged with a rubber septum. The capillary was heated at 74°C for 24 h. Subsequently the BMA-EDMA column was flushed with acetonitrile and blown dry with nitrogen gas. The BuMa column was cut to a final length of 4.5 cm and used as a precolumn.

2.5 Column switching system

LC separations were initially carried out using an Agilent (Santa Clara, CA, USA) 1200 nanopump. Mobile phases used for gradient separations consisted of A (0.1% FA in water) and B (0.1% FA, 10% water in acetonitrile). A 4.5 cm BuMa precolumn was connected between two PEEK T-pieces (Upchurch Scientific, Oak Harbor, WA, USA) each with a sweep volume of 29 nL. Samples were injected using a Valco (VICI Valco Instruments, Huston, TX, USA) injector with a 500 nL internal loop. The sample was loaded into the 50 μm id precolumn for 2.5 min at a flow rate of 0.5 μL/min (Fig. 1). Prior to onset of solvent gradient, the six-port valve was switched and the pump flow was increased to 2 μL/min. This valve position enabled a flow splitting before the precolumn resulting in appropriate separation flow rates through the pre and analytical columns (20 to 80 nL/min were examined in this study). Note that this splitting does not affect the volume injected, as the whole 500 nL entered the precolumn during sample loading (Supporting Information Fig. S3). To measure the flow rates through the PLOT columns, 50 and 75 μm id fused-silica capillaries were connected to the end of the 10 μm i.d. PLOT columns with a PicoClear union (New Objective, Woburn, MA, USA). The liquid was allowed to flow into the measuring capillaries for a given time, and the length traveled was visually measured and used to calculate the flow rate (Supporting Information Fig. S4). For ESI-MS, a distal-coated pulled-tip nanospray needle (20 μm id

with 5 μm id orifice, New Objective) was cut shorter to reduce post column volume (about 12–15 nL in the needle after cutting) and connected to the end of the PLOT column using a PicoClear union. In BxPC3 protein identification experiments, the columns, parts and settings described above were incorporated in an Easy 1000 nLC system (Thermo Fisher Scientific, Waltham, MA, USA), with the exception of the flow rate before splitting (200 nL/min) and injection volume (1 μL).

2.6 Mass spectrometric detection, data extraction, and identification

A Q-Exactive Orbitrap MS (Thermo) equipped with a nanospray ESI source was used for mass spectrometric detection. An electrospray was created using a spray voltage of 2.1 kV and mass spectra were acquired from m/z 400 to 1500 in the positive ion mode. The AGC target was set to 2e5 ions. Data were acquired at a resolution of 35 000 and the scan speed with the setting used was 7.2 scans per second. Extracted ion chromatograms (EICs) were obtained using $\Delta m/z$ of 20 ppm.

For MS/MS analysis of BxPC3 cells, a spray voltage of 1.5 kV was used, with a scan range of m/z 350–1850 in the positive ion mode. The top ten highest intensity ions were fragmented in each spectrum, with the exception of singly charged ions, and ions with a charge above six. The AGC target and resolution were set to 5e6, 70 000 in MS and 5e5, 35 000 in MS/MS, respectively. A high-energy collision dissociation was performed with a normalized collision energy of 25%.

The identification of BxPC3 proteins was performed using Proteome Discoverer v1.3 (Thermo Scientific) by combining the SEQUEST and Mascot algorithms. Mascot and SEQUEST searches were performed against the SwissProt database with human taxonomy and the human protein database (www.uniprot.org), respectively. Enzyme specificity was set to trypsin, and a maximum of two missed cleavages were allowed. The precursor mass tolerance was set to 15 ppm (MS) and the fragment tolerance to 20 mmu (MS/MS). Carbamiodomethylation of cysteine, oxidation of methionine and phosphorylation of serine, threonine, and tyrosine were set as dynamic modifications. The false discovery rate was determined by searching against a decoy database and a strict value of 0.01 was applied. Peptide spectral match was set to medium, and only Peptide spectral matches better than 0.15 were considered as a positive peptide match.

2.7 Peak capacity calculations

Peak capacity calculations were based on a previously described definition [25];

$$nc^{**} = (t_{\text{first}} - t_{\text{last}})/W_{\text{av}} \quad (1)$$

where t_{first} and t_{last} are the retention times of the first and last eluting peptides in the sample, and W_{av} is the average peak widths of the extracted peaks within the selected retention window. Peak widths were measured at 10% of the peak height ($W_{0.1}$) in the EICs and the retention window was calculated from the first and last eluting peptide, as previously described [21]. For the peak capacity calculations based on separations of tryptic digested cytochrome c in the present study, five peptide m/z values spread over the retention window were extracted for each chromatogram.

3 Results and discussion

3.1 Preparation of long PLOT columns with decreased backpressure

Recently, several groups have packed or synthesized very long LC columns for maximizing peak capacity [26–28], as this is often correlated with the number of proteins that can be identified based on LC–MS/MS data [6]. Long columns can be packed with particles, but such columns generate high backpressures [29] and are difficult to pack in narrow formats [30]. Regarding highly permeable monolithic columns, the preparation often requires a mixture of two or three solvents to serve as the porogenic solution. The ratio of these solvents is of major importance regarding morphology and the resulting backpressure [31], and small deviations may result in low chromatographic performance, production repeatability, or clogged columns. In this regard, a major advantage of the PS-DVB PLOT column preparation is the use of a single solvent in the polymerization solution. We have prepared about 15 10 μm id (and some 5 and 20 μm id) PLOT columns, and our experience is that these columns are easier to produce reproducibly compared to organic monolithic columns independent of the person making the column (for more details on column-to-column repeatability, see [18, 19]). To manufacture long 10 μm id PLOT columns, a simple pressure bomb system coupled directly to a gas flask was developed (Supporting Information Fig. S1). Column lengths were however limited to about 6 m, due to the maximum pressure of 200 bar in these gas flasks. To enable production and use of longer PLOT columns and higher flow rates than previously described, columns with reduced backpressure were produced. A polymerization solution containing 70% ethanol and 30% monomers was used, giving a layer thickness of about 0.70–0.75 μm. Hence, the columns had a larger interstitial zone, reducing the column backpressure compared to previously described 1 μm layer PLOT columns [19]. Even with the reduced stationary phase thickness, the loadability of 120 fmol (Supporting Information Fig. S5) was not reduced compared to that previously reported with a 1 μm layer column (~100 fmol). We believe that the high loadability is due to the effective SPE to LC transfer compared to pressure bomb driven injections used earlier [18]. The loadability is of course lower compared to larger sized columns, but surprisingly comparable to commercial nanocolumns, e.g. that in [32].

Nonetheless, it should be kept in mind that very limited sample analysis is the most natural application area of PLOT columns.

3.2 A simple column switching system

In our previously reported 10 μm id PLOT-LC system [19] for intact protein separation, a simple split system was used to show a proof of principle. A major drawback was that the flow split was placed after the injector and before the PLOT column, leading 99% of the sample directly to waste, and only 1% onto the PLOT column. Coupling with an enrichment column allows faster sample loading, the possibility of loading larger sample volumes and less column clogging, and has previously been successfully used with 10 μm id PLOT columns [20, 33, 34]. However, the system in these studies consisted of one ten- and one six-port valve and three T-pieces (one of which is not commercially available), and required flow splitting both during sample loading and gradient separation. We therefore designed and utilized a simpler design (Fig. 1), compatible with common nano-LC systems (e.g. the Thermo Easy-nLC or the Waters nanoAcquity), consisting of only one six-port switching valve and only commercially available parts. The only difference between our system and common nano-LC systems is that the union between the pre and analytical columns is T-coupled with a "gradient split" fused-silica capillary. Splitting the flow at this junction during the LC separation step significantly reduces the gradient delay time, and allows stable flow rates down to 20 nL/min through the columns during gradient separation.

To evaluate the repeatability of this simple system, three consecutive injections and separations were performed using a 25 μg/mL transferrin tryptic digest (Supporting Information Table S1). The retention time RSDs were $\leq$0.2%. Thus, we were in a position to further evaluate important separation parameters such as flow rate, column length and gradient times, with the goal of maximizing the separation power of the simplified PLOT-LC system.

3.4 Effect of flow rate, gradient times, and temperature

PLOT columns have previously been shown to have potential for high-resolution separations [18], but an empirical exploration of the key parameters to locate maximum peak capacity settings has not been described. Tryptic digests of cytochrome c were chromatographed at 20, 40, 60, and 80 nL/min, at gradient times of 30, 60, 90, 120, 150, 180 min on a 2.4 m PLOT column using the above-described column switching system. The mobile phase gradient was from 5 to 71% B in all cases. A high gradient steepness was used to elute all peptides within a 30 min t_G at 20 nL/min. Flow rates below 20 nL/min were not evaluated, as this was the minimum recommended flow rate for stable nanospray using commercial spray needles with a 5 μm id orifice. Peptide signal intensities were found to vary less than ten percent in the range of flow rates studied. For evaluating the resolving power of the various combinations, the stringent n_c** definition of peak capacity (compared to, e.g. t_G/W_{av}) was used to avoid misinterpretations, e.g. overestimating peak capacities in the case of short retention windows relative to gradient length. Peak width was defined as the width at 10% of peak height. This should ensure a more realistic assessment of the number of compounds that can be separated during the gradient, taking more into account nonideal/Gaussian peak shapes as, e.g. tailing effects, compared with using 2σ, or $W_{0.5}$. Recent theoretical calculations for OT-LC optimization predicted higher performance at elevated temperatures [8]. However, elevated temperatures (40–90°C) resulted in significant signal reductions (at 40 nL/min, Supporting Information Fig. S6). This is in agreement with previous PLOT/temperature experiments at these low flow rates (20 nL/min) [19] and seems to be independent of the type of electrospray source. We speculate that this may be due to more poorly charged droplet formation at elevated temperatures at these low flow rates. Therefore, column temperatures were kept ambient. The peak capacity increased with longer gradient times, as expected (Fig. 2A). For the 2.4 m column, the peak capacity approached a limiting value at gradient times between 150 and 180 min. The highest values for the column switching system were obtained at 40 nL/min (corresponding to ~12 mm/s when subtracting a 0.75 μm layer thickness in the 10 μm id column) followed by 20 nL/min (6 mm/s). At 60 nL/min (18 mm/s), the peak capacity dropped significantly compared to the lower flow rates, and 80 nL/min (24 mm/s) gave in general the lowest values. This trend is quite different from that previously reported on a PS-DVB monolith with a similar experiment, where peak capacity increased continuously with increasing flow rate and t_G [35]. Also, as seen in Fig. 3A, the decrease in peak capacity at elevated flow rates was more significantat longer gradient times (e.g. 180 min) compared to shorter gradient times, similar to the findings of Wang et al. for packed columns [25]. Figure 2B shows that the retention window is relatively unchanged for all flow rates, since both the first and the last eluting peptide appear earlier in the chromatogram, as expected from theory [25]. More importantly, the W_{av} decreased when the flow rate was increased from 20 to 40 nL/min, but increased more at higher flow rates. These results are similar to monoliths with large macropores (up to 10 μm) where a large mass-transfer resistance at elevated flow rates has been reported [36], and this is explained by the large distance between the solid structures containing the stationary phase [37], similar to the inner diameter of OT columns. In summary, 40 nL/min appeared to be the optimal flow rate for the 10 μm id regarding chromatographic performance and nanospray stability.

3.5 Column length and gradient times

Columns of 2.4, 5.4, and 8.0 m were used at a flow rate of 40 nL/min with gradient elution from 5 to 40% B with

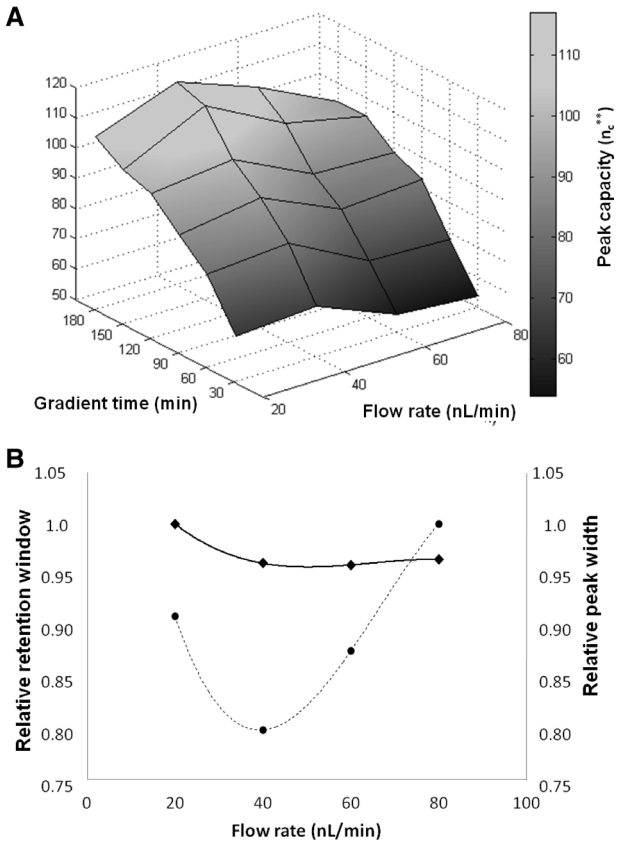

Figure 2. (A) Effect of flow rate and t_G on peak capacity using a 2.4 m long 10 μm id PLOT column in the column switching system. Solvent gradients were from 5 to 71% B at flow rates from 20 to 80 nL/min. (B) Relative retention window (solid line, and diamonds) and peak width (dashed line and circles) as function of flow rate at a t_G of 180 min. Relative values were calculated from 58 min and 35 s for retention window and peak width, respectively. Peak widths were measured at $W_{0.1}$ and the average value for five peptide peaks spread over the retention window were used for calculating the peak capacities using Eq. (1), as described in Section 2.

gradient times from 40 to 490 min, except the combinations of (2.4 m, 490 min) and (8.0 m, 40 min; Fig. 3). The 8 m column was made by connecting a 2.6 and a 5.4 m column in series with a PicoClear union. As expected, the lowest peak capacities were obtained with the shortest column, while an increase in length to 5.4 m gave a significant increase in performance. A more moderate gain was obtained by increasing the column length to 8 m. The lower increase in peak capacity for longer columns is not surprising since peak capacity is expected to increase with the square root of the column length [38, 39]. The increase in peak capacities with column length corresponds well with theory; the observed increase from 2.4 to 5.4 m and from 5.4 to 8.0 were only 4% larger and 8% lower than predicted, respectively. The slightly lower increase than predicted from theory for the 8.0 m column may be due to small extra-column volume because two columns were connected to obtain the 8.0 m column. Interestingly, the shortest column was outperformed even at short gradient times (40 and 80 min). This reduced performance could be due to

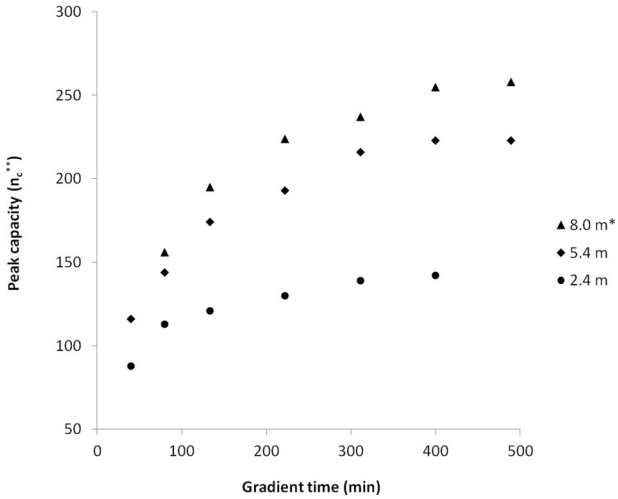

Figure 3. Peak capacity as a function of t_G and the column length. The gradient used was from 5 to 40% B at a flow rate of 40 nL/min. *The 8 m column was made by connecting a 2.6 and 5.4 m column in series using a PicoClear union.

extra-column volumes of the SPE–LC system. However; the low performance of short PLOT columns has also previously been observed (for intact proteins) using column lengths of 1 and 2 m, using a system without SPE trapping [19]. The maximum column length with backpressures comfortably below the limits of the pumps and connections employed was about 8 m. Longer columns could be employed, but at the cost of significantly longer analysis time and higher pressures and rather moderate gains in peak capacity. Theoretically, for a 21 m column, the backpressure would be ~1000 bar, with an expected 63% increase in peak capacity compared to the 8 m column. Although a t_G of 490 min provided the highest peak capacity, the gain was considered insignificant compared to the shorter 400 min gradient. In summary, 40 nL/min flow rate, using an 8 m long column and a t_G of 400 min was for all practical purposes considered as optimal for the 10 μm id PLOT columns.

With these settings, a peak capacity of at least 415 was achieved when injecting about 23 ng of an in-gel-tryptic-digested gel fraction from rat liver (Fig. 4A), calculated using EICs from the seven peptides shown in Fig. 4B (average $W_{0.1}$ was 0.82 min). Higher peak capacities were obtained for the gel digest compared to the cytochrome c digest due to the larger retention window, because of a larger range of hydrophobicity of peptides in the more complex mixture. In order to compare the results achieved with the optimized PLOT system with peak capacities reported by others, the peak widths have to be measured in the same way. We therefore measured and calculated peak capacities for the rat liver sample by measuring at peak heights as defined in references [18, 28, 40]. Using peak width = 2σ in the n_c** formula (Eq. (1)), Yue et al. reported PLOT peak capacities of 400 [18]. With the same criteria, we obtained a 2.3-fold increase (950) using our optimized settings. Iwasaki et al. showed a peak capacity of ~680 (using peak width = $W_{0.5}$

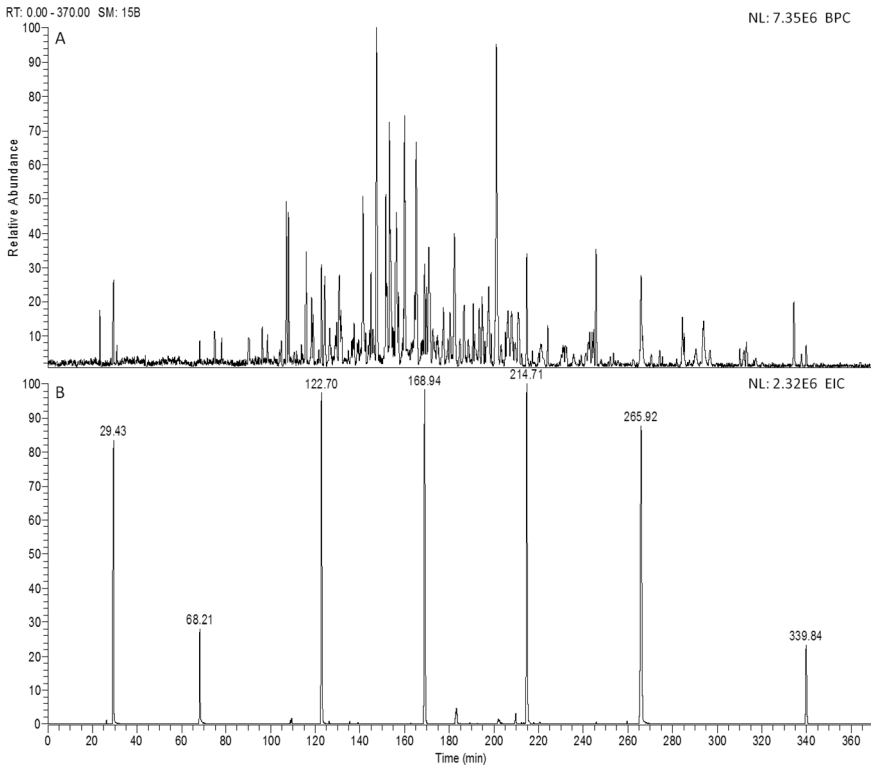

Figure 4. Base peak chromatogram of the separation of an in-gel-digested fraction of a rat-liver sample using a 4.5 cm × 50 μm id BuMa monolithic column as pre-column and an 8 m long × 10 μm id PS-DVB PLOT column (A). EICs of seven high-intensity peptide peaks used for peak capacity calculation (m/z = 747.3537, 788.3969, 805.9422, 815.9759, 961.7538, 996.1733, 1045.5761) (B). About 23 ng tryptic digest from a SDS-PAGE cut (~50 kDa fraction). The gradient used was from 5 to 40% mobile phase B in 400 min at a flow rate of 40 nL/min. The 8 m PLOT column was made by connecting a 5.4 and 2.6 m PLOT column in series using a PicoClear connector. The maximum pressure during the gradient was 375 bar.

in, Eq. (1)) [40]. Using the same criteria, we reached a substantially higher capacity (791). Similar peak capacities (~410, measuring at 4σ) can be obtained with long nanocolumns packed with sub 2 μm porous particles, but requiring ultra-high pressures (e.g. 1200 bar) [28]. Recent efforts using 2.1 mm id core–shell particle columns have also achieved higher peak capacities (1360 calculated using t_G and 4σ), but these columns are operated at 1200 bar, and are not as suited for trace analysis or limited sample amounts [41].

3.6 Analysis of slow cycling cancer cells

As our work often revolves around analysis of limited samples (e.g. cancer cells with stem-like properties or very slow cycling cells) related to cell signaling, the developed PLOT-LC methodology was assessed by analyzing limited amounts of trypsin-cleaved peptides from BxPC3 β catenin (−/−) cells, a very slow growing cell line. When injecting extract from just 1000 cells, the system could identify up to 456 proteins per analysis (1958 peptides). With this limited sample amount, we were able to detect a valuable number of central Wnt pathway members or regulators, e.g. tankyrase-2, a low-abundance regulator of the β catenin destruction complex (Fig. 5) and key player in therapeutic Wnt/β catenin targeting [42], and moesin and flap endonuclease 1, proteins that have just recently been discovered of having effects on the pathway [43, 44]. Figure 6 shows a map of identified Wnt regulators and points of interaction with other members of the pathway (for further details, see Supporting Information Table S2). When injecting extract from 10 000 cells, 6770 peptides from 1187 proteins were identified (937 identified with a minimum of two peptides), also in just one single injection. For 100 000 cell injections, 12 134 peptides from 2310 proteins could be identified (1529 identified with a minimum of two peptides). Even higher numbers of identified proteins with such limited samples can be expected by combining cleavage reagents (i.e. lys C and trypsin [45]). Carry-over can often haunt peptide analysis, but in the current system carry-over was considered low (average ≤0.6%), assessed by comparing peak areas of high abundant peptides present in the BxPC3 β catenin (−/−) samples and subsequent blank injections. We believe that low carry-over is a trait of PLOT columns, as we previously also found this to be the case with intact proteins [19].

4 Conclusion

We have developed a simple PLOT-LC system that is fully compatible with the hardware of commercial nano-LC instrumentation, without additional hardware or custom-made fittings. The current system enabled analysis of the whole injected sample, without sample splitting. As result of a systematic study, the optimal separation parameters at conventional pressures (<400 bar) were a flow rate of 40 nL/min in combination with an 8 m column length at a t_G of 400 min. The optimized method achieved a peak capacity of 791 or 415 using $W_{0.5}$ or $W_{0.1}$, respectively, doubling the peak capacity achieved in earlier PLOT studies, and meeting or surpassing

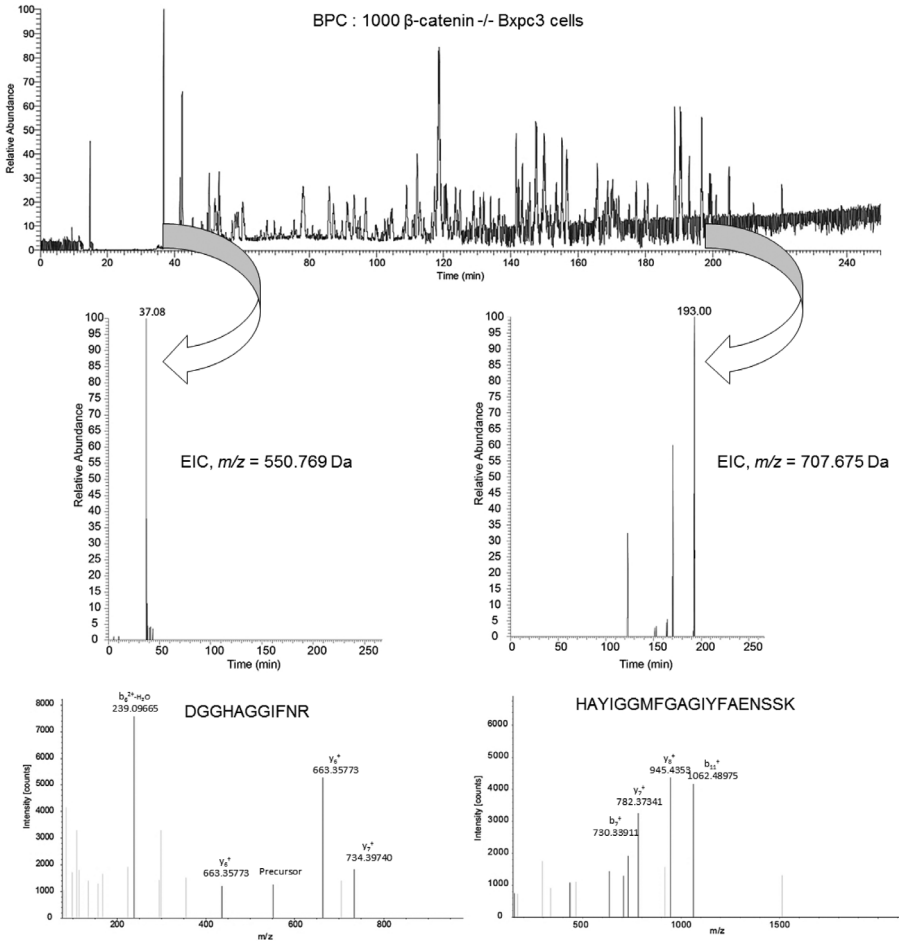

Figure 5. Top: base peak chromatogram from the analysis of extract corresponding to 1000 BxPC3 cells. Middle: EIC of two tryptic tankyrase-2 peptides. Bottom: fragment mass spectrum of the two tankyrase peptides. Column length, flow rate, and solvent gradient as in Fig. 4.

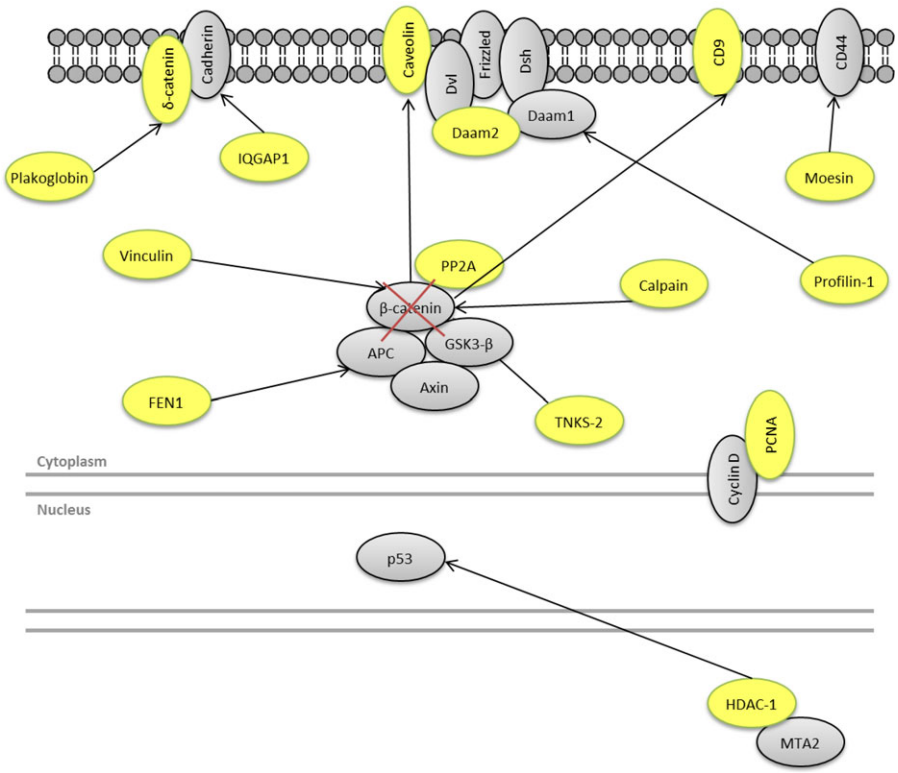

Figure 6. Overview of identified Wnt-signaling pathway proteins (yellow) in extract corresponding to 1000 β catenin (−/−) cells and sites of interaction with other Wnt proteins. For more details, see Supporting Information Table S2.

capacities achieved in recent studies using monolith or UHPLC based nanocolumns. The peak capacities of these PLOT columns are expected to be improved further in combination with UHPLC equipment, as longer columns can be used. The current set-up was fully automated with a commercial nanopump for the analysis of slow cycling cancer cells, where 456 proteins (1958 peptides) were identified from the analysis of only 1000 cells, allowing detection of a significant number of members and regulators of the Wnt signal pathway. When increasing number of cells analyzed, ~2300 proteins could be identified in just one single run. This encourages us to employ PLOT LC in our further work with limited samples related to our Wnt studies (e.g. microdissection and cell subpopulation studies). Although OT-LC columns were relatively newly "reintroduced", their chromatographic performance is already in the same league as far more established column materials where production and separation conditions have been being optimized for almost two decades. We expect the potential of OT columns to be further realized as new stationary phases are being developed (e.g. [46–49]), as well as our ongoing development and testing of novel PLOT stationary phases.

The in-gel tryptic digested rat liver fraction was prepared by Anders Moen (Institute of Molecular Bioscience, University of Oslo). The Bxpc3 β catenin (−/−) cell line was acquired from Dr. Petter Angell Olsen (Oslo University Hospital, Oslo, Norway). The Norwegian Research Council is greatly acknowledged for financial support through the research grant 197431/F20.

The authors have declared no conflict of interest.

5 References

[1] Smith, R. D., Shen, Y., Tang, K., *Acc. Chem. Res.* 2004, *37*, 269–278.

[2] Shen, Y., Zhao, R., Berger, S. J., Anderson, G. A., Rodriguez, N., Smith, R. D., *Anal. Chem.* 2002, *74*, 4235–4249.

[3] Wang, Y., Rudnick, P. A., Evans, E. L., Li, J., Zhuang, Z., DeVoe, D. L., Lee, C. S., Balgley, B. M., *Anal. Chem.* 2005, *77*, 6549–6556.

[4] Trouillon, R., Passarelli, M. K., Wang, J., Kurczy, M. E., Ewing, A. G., *Anal. Chem.* 2013, *85*, 522–542.

[5] Nguyen, L. V., Vanner, R., Dirks, P., Eaves, C. J., *Nat. Rev. Cancer* 2012, *12*, 133–143.

[6] Koecher, T., Swart, R., Mechtler, K., *Anal. Chem.* 2011, *83*, 2699–2704.

[7] Fairchild, J. N., Walworth, M. J., Horvath, K., Guiochon, G., *J. Chromatogr. A* 2010, *1217*, 4779–4783.

[8] Causon, T. J., Shellie, R. A., Hilder, E. F., Desmet, G., Eeltink, S., *J. Chromatogr. A* 2011, *1218*, 8388–8393.

[9] Swart, R., Kraak, J. C., Poppe, H., *Trends Anal. Chem.* 1997, *16*, 332–342.

[10] Tsuda, T., Hibi, K., Nakanishi, T., Takeuchi, T., Ishii, D., *J. Chromatogr.* 1978, *158*, 227–232.

[11] Bruin, G. J. M., Stegeman, G., Van, A. A. C., Xu, X., Kraak, J. C., Poppe, H., *J. Chromatogr.* 1991, *559*, 163–181.

[12] Guiochon, G., *J. Chromatogr. A* 2006, *1126*, 6–49.

[13] Jorgenson, J. W., Guthrie, E. J., *J. Chromatogr.* 1983, *255*, 335–348.

[14] Kucera, P., Guiochon, G., *J. Chromatogr.* 1984, *283*, 1–20.

[15] Eguchi, S., Kloosterboer, J. G., Zegers, C. P. G., Schoenmakers, P. J., Tock, P. P. H., Kraak, J. C., Poppe, H., *J. Chromatogr.* 1990, *516*, 301–312.

[16] Moseley, M. A., Deterding, L. J., De, W. J. S. M., Tomer, K. B., Kennedy, R. T., Bragg, N., Jorgenson, J. W., *Anal. Chem.* 1989, *61*, 1577–1584.

[17] Hulthe, G., Petersson, M. A., Fogelqvist, E., *Anal. Chem.* 1999, *71*, 2915–2921.

[18] Yue, G., Luo, Q., Zhang, J., Wu, S.-L., Karger, B. L., *Anal. Chem.* 2007, *79*, 938–946.

[19] Rogeberg, M., Wilson, S. R., Greibrokk, T., Lundanes, E., *J. Chromatogr. A* 2010, *1217*, 2782–2786.

[20] Luo, Q., Yue, G., Valaskovic, G. A., Gu, Y., Wu, S.-L., Karger, B. L., *Anal. Chem.* 2007, *79*, 6174–6181.

[21] Rogeberg, M., Wilson, S. R., Malerod, H., Lundanes, E., Tanaka, N., Greibrokk, T., *J. Chromatogr. A* 2011, *1218*, 7281–7288.

[22] Moen, A., Hafte, T. T., Tveit, H., Egge-Jacobsen, W., Prydz, K., *Glycobiology* 2011, *21*, 1416–1425.

[23] Courtois, J., Szumski, M., Bystroem, E., Iwasiewicz, A., Shchukarev, A., Irgum, K., *J. Sep. Sci.* 2006, *29*, 14–24.

[24] Geiser, L., Eeltink, S., Svec, F., Frechet, J. M. J., *J. Chromatogr. A* 2007, *1140*, 140–146.

[25] Wang, X., Stoll, D. R., Schellinger, A. P., Carr, P. W., *Anal. Chem.* 2006, *78*, 3406–3416.

[26] Eghbali, H., Sandra, K., Detobel, F., Lynen, F., Nakanishi, K., Sandra, P., Desmet, G., *J. Chromatogr. A* 2011, *1218*, 3360–3366.

[27] Iwasaki, M., Sugiyama, N., Tanaka, N., Ishihama, Y., *J. Chromatogr. A* 2012, *1228*, 292–297.

[28] Cristobal, A., Hennrich, M. L., Giansanti, P., Goerdayal, S. S., Heck, A. J. R., Mohammed, S., *Analyst* 2012, *137*, 3541–3548.

[29] Shen, Y., Zhang, R., Moore, R. J., Kim, J., Metz, T. O., Hixson, K. K., Zhao, R., Livesay, E. A., Udseth, H. R., Smith, R. D., *Anal. Chem.* 2005, *77*, 3090–3100.

[30] Luo, Q., Page, J. S., Tang, K., Smith, R. D., *Anal. Chem.* 2007, *79*, 540–545.

[31] Svec, F., *J. Sep. Sci.* 2004, *27*, 747–766.

[32] Dolman, S., Eeltink, S., Vaast, A., Pelzing, M., *J. Chromatogr. B* 2013, *912*, 56–63.

[33] Thakur, D., Rejtar, T., Wang, D., Bones, J., Cha, S., Clodfelder-Miller, B., Richardson, E., Binns, S., Dahiya, S., Sgroi, D., Karger, B. L., *J. Chromatogr. A* 2011, *1218*, 8168–8174.

[34] Wang, D., Hincapie, M., Rejtar, T., Karger, B. L., *Anal. Chem.* 2011, *83*, 2029–2037.

[35] Detobel, F., Broeckhoven, K., Wellens, J., Wouters, B., Swart, R., Ursem, M., Desmet, G., Eeltink, S., *J. Chromatogr. A* 2010, *1217*, 3085–3090.

[36] Ishizuka, N., Minakuchi, H., Nakanishi, K., Soga, N., Nagayama, H., Hosoya, K., Tanaka, N., *Anal. Chem.* 2000, *72*, 1275–1280.

[37] Gzil, P., Vervoort, N., Baron, G. V., Desmet, G., *Anal. Chem.* 2004, *76*, 6707–6718.

[38] van de Meent, M. H. M., de Jong, G. J., *J. Sep. Sci.* 2009, *32*, 487–493.

[39] Wang, X., Barber, W. E., Carr, P. W., *J. Chromatogr. A* 2006, *1107*, 139–151.

[40] Iwasaki, M., Miwa, S., Ikegami, T., Tomita, M., Tanaka, N., Ishihama, Y., *Anal. Chem.* 2010, *82*, 2616–2620.

[41] De, V. J., Stassen, C., Vaast, A., Desmet, G., Eeltink, S., *J. Chromatogr. A* 2012, *1264*, 57–62.

[42] Huang, S.-M. A., Mishina, Y. M., Liu, S., Cheung, A., Stegmeier, F., Michaud, G. A., Charlat, O., Wiellette, E., Zhang, Y., Wiessner, S., Hild, M., Shi, X., Wilson, C. J., Mickanin, C., Myer, V., Fazal, A., Tomlinson, R., Serluca, F., Shao, W., Cheng, H., Shultz, M., Rau, C., Schirle, M., Schlegl, J., Ghidelli, S., Fawell, S., Lu, C., Curtis, D., Kirschner, M. W., Lengauer, C., Finan, P. M., Tallarico, J. A., Bouwmeester, T., Porter, J. A., Bauer, A., Cong, F., *Nature* 2009, *461*, 614–620.

[43] Zhu, X., Morales, F. C., Agarwal, N. K., Dogruluk, T., Gagea, M., Georgescu, M.-M., *Cancer Res.* 2013, *73*, 1142–1155.

[44] Jaiswal, A. S., Armas, M. L., Izumi, T., Strauss, P. R., Narayan, S., *Neoplasia* 2012, *14*, 495–508.

[45] Glatter, T., Ludwig, C., Ahrne, E., Aebersold, R., Heck, A. J. R., Schmidt, A., *J. Proteome Res.* 2012, *11*, 5145–5156.

[46] Forster, S., Kolmar, H., Altmaier, S., *J. Chromatogr. A* 2013, *1283*, 110–115.

[47] Forster, S., Kolmar, H., Altmaier, S., *J. Chromatogr. A* 2012, *1265*, 88–94.

[48] Collins, D. A., Nesterenko, E. P., Brabazon, D., Paull, B., *Analyst* 2013, *138*, 2540–2545.

[49] Nesterenko, E., Yavorska, O., Macka, M., Yavorskyy, A., Paull, B., *Anal. Methods* 2011, *3*, 537–543.

